Research Article | Vol 25, No. 11 | 29 May 2017 | OPTICS EXPRESS 12867
Optics EXPRESS

# Optical compensation for the perturbed three mirror anastigmatic telescope based on nodal aberration theory

XIAOBIN ZHANG,[1,2,*] SHUYAN XU,[1] HONGCAI MA,[1] AND NANNAN LIU[1]

[1]*Changchun Institute of Optics, Fine Mechanics and Physics, Chinese Academy of Science, Changchun 130033, China*
[2]*University of Chinese Academy of Science, Beijing 100049, China*
[*]*hitzhangxiaobin@163.com*

**Abstract:** In this paper, the Zernike coefficient is analytically expressed as the product of the dependence of aberration field decenter vectors (related with perturbations) and the dependence of fields of view (FOVs), on the frame work of nodal aberration theory (NAT). By expanding and analyzing this expression, an alignment strategy by optical compensation for the perturbed on-axis or off-axis telescope is presented. Specifically, two cases, corresponding to the misalignment of tertiary mirror (TM) and the deformation of primary mirror (PM), respectively, are discussed for the same three mirror anastigmatic (TMA) telescope. Here the misaligned TM and the deformed PM are compensated only by aligning secondary mirror (SM). By analyzing the aberration field after compensation with the nominal, it is found that either PM or TM can be compensated by SM. It is also found TM is more easily compensated than PM. In the end, the NAT method developed here used for optical compensation is compared to merit function regression (MFR) method and sensitivity table method (STM). By comparing NAT method with MFR method, it is shown that the calculated correction values of SM based on NAT method is very close to the referred values obtained from MFR method. It proves the correctness of NAT method developed here. By comparing NAT method with STM, it demonstrates that the computation accuracy of NAT method is much higher in poor conditions and NAT method is less sensitive to measurement errors. It is further illustrated that the theory of optical compensation by SM developed here is correct and applicable.



**OCIS codes:** (080.1005) Aberration expansions; (220.1000) Aberration compensation; (110.6770) Telescopes; (220.1140) Alignment; (220.1080) Active or adaptive optics.

## References and links

1. S. G. L. Williams, "On-axis three-mirror anastigmat with an offset field of view," Proc. SPIE **183**, 212–217 (1979).
2. M. Lampton and M. Sholl, "Comparison of on-axis three-mirror-anastigmat telescopes," Proc. SPIE **6687**, 66870S (2007).
3. L. G. Cook, "Three-mirror anastigmat used of-axis in aperture and field," Proc. SPIE **183**, 207–211 (1979).
4. J. Robichaud, M. Anapol, L. Gardner, and P. Hadfield, "Ultralightweight off-axis three-mirror anastigmatic SiC visible telescope," Proc. SPIE **2543**, 180–184 (1995).
5. P. Davila, B. Bos, J. Contreras, C. Evans, M. Greenhouse, G. Hobbs, W. Holota, L. W. Huff, J. Hutchings, T. H. Jamieson, P. Lightsey, C. Morbey, R. Murowinski, M. Rieke, N. Rowlands, B. Steakley, M. Wells, M. T. Plate, and D. G. Wright, "The James Webb Space Telescope science instrument suite: an overview of optical designs," Proc. SPIE **5487**, 611–627 (2004).
6. R. N. Wilson, F. Franza, and L. Noethe, "Active optics: I. A system for optimizing the optical quality and reducing the costs of large telescopes," J. Mod. Opt. **34**(4), 485–509 (1987).
7. M. Liang, V. Krabbendam, C. F. Claver, S. Chandrasekharan, and B. Xin, "Active Optics in Large Synoptic Survey Telescope," Proc. SPIE **8444**, 84444Q (2012).
8. J. M. Howard, "Optical modeling activities for NASA's James Webb Space Telescope (JWST): III. Wavefront aberrations due to alignment and figure compensation," Proc. SPIE **6675**, 667503 (2007).
9. J. M. Howard, K. Q. Ha, R. Shiri, J. S. Smith, G. Mosier, and D. Muheim, "Optical modeling activities for NASA's James Webb Space Telescope (JWST): Part V. Operational alignment updates," Proc. SPIE **7071**, 70710X (2008).

#291029 https://doi.org/10.1364/OE.25.012867
Journal © 2017 Received 20 Mar 2017; revised 12 May 2017; accepted 15 May 2017; published 24 May 2017

Optics EXPRESS

10. E. D. Kim, Y. W. Choi, M. S. Kang, and S. C. Choi, "Reverse-optimization alignment algorithm using Zernike sensitivity," J. Opt. Soc. Korea **9**(2), 68–73 (2005).
11. S. Kim, H. S. Yang, Y. W. Lee, and S. W. Kim, "Merit function regression method for efficient alignment control of two-mirror optical systems," Opt. Express **15**(8), 5059–5068 (2007).
12. G. Ju, C. Yan, Z. Gu, and H. Ma, "Computation of astigmatic and trefoil figure errors and misalignments for two-mirror telescopes using nodal-aberration theory," Appl. Opt. **55**(13), 3373–3386 (2016).
13. Z. Gu, C. Yan, and Y. Wang, "Alignment of a three-mirror anastigmatic telescope using nodal aberration theory," Opt. Express **23**(19), 25182–25201 (2015).
14. J. Sebag, W. Gressler, T. Schmid, J. P. Rolland, and K. P. Thompson, "LSST Telescope Alignment Plan Based on Nodal Aberration Theory," Publ. Astron. Soc. Pac. **124**(914), 380–390 (2012).
15. B. Jiang, S. Z. Zhou, K. Jiang, H. Y. Fu, and C. Mei, "Alignment off-axis optical system using Nodal Aberration Theory," Proc. SPIE **8910**, 89100E (2013).
16. X. Zhang, D. Zhang, S. Xu, and H. Ma, "Active optical alignment of off-axis telescopes based on nodal aberration theory," Opt. Express **24**(23), 26392–26413 (2016).
17. K. Thompson, "Description of the third-order optical aberrations of near-circular pupil optical systems without symmetry," J. Opt. Soc. Am. A **22**(7), 1389–1401 (2005).
18. K. P. Thompson, T. Schmid, O. Cakmakci, and J. P. Rolland, "Real-ray-based method for locating individual surface aberration field centers in imaging optical systems without rotational symmetry," J. Opt. Soc. Am. A **26**(6), 1503–1517 (2009).
19. R. Tessieres, "Analysis for alignment of optical systems," Ph.D. dissertation (University of Arizona, Tucson, Arizona, 1980).
20. R. A. Buchroeder, "Tilted component optical systems," Ph.D. dissertation (University of Arizona, Tucson, Arizona, 1976).
21. T. Schmid, "Misalignment Induced Nodal Aberration Fields and Their Use in the Alignment of Astronomical Telescopes," Ph.D. dissertation (University of Central Florida Orlando, Florida, 2010).
22. R. W. Gray and J. P. Rolland, "Wavefront aberration function in terms of R. V. Shack's vector product and Zernike polynomial vectors," J. Opt. Soc. Am. A **32**(10), 1836–1847 (2015).
23. T. Schmid, J. P. Rolland, A. Rakich, and K. P. Thompson, "Separation of the effects of astigmatic figure error from misalignments using nodal aberration theory (NAT)," Opt. Express **18**(16), 17433–17447 (2010).

## 1. Introduction

Compared to other classes of astronomical telescopes, three mirror anastigmatic (TMA) telescopes, either on-axis [1,2] or off-axis [3,4], own less optical elements while maintaining perfect optical performance. For this reason, the main optical system of some astronomical telescopes is designed as TMA type. The famous one is JWST [5]. Generally, the image quality of astronomical telescopes is always required to be perfect in operating condition. But astronomical telescopes are easily perturbed because of vibration, thermal variation and other factors, resulting that the image quality is severely degraded. To maintain the image quality, the perturbed telescope needs to be aligned on orbit, which can be realized by integrating an active optical system.

In active optics [6,7], the optimal alignment strategy is system recovery, which means the aligned system is same as the designed. To realize it, all the optical elements must have adjustment mechanisms. It is ill-considered in the engineering. Actually, there is no need to equip adjusting mechanism with every optical element. The purpose of optical alignment in active optics is to optimize the image quality of the perturbed telescope, which can also be realized by system compensation [8,9]. For TMA telescopes, the size of secondary mirror (SM) is much smaller than that of primary mirror (PM) and tertiary mirror (TM). So SM is more easily adjusted. If the perturbed system can be compensated to meet the required optical performance by SM, then only SM needs to be adjusted. It is the most practical alignment strategy.

To finish system compensation, the correction values (adjusting values) should be first determined. To determine these correction values, several alignment algorithms have been studied, for instance, sensitivity table method (STM), merit function regression (MFR) method and nodal aberration theory (NAT) method. Among them, STM [10], which is based on the sensitivity of perturbation parameters to wave-front, is commonly used (including Zernike coefficient sensitivity, RMS wave-front error sensitivity, MTF sensitivity). In this method, all the sensitivities are linear approximate. If the perturbed wave-fronts are linearly varying to perturbations with respect to the nominal wave-front, the calculated perturbations

Optics EXPRESS

based on STM are accurate. But with the increase of perturbation ranges, the linear relationship between them will be broken, resulting that the calculated perturbations based on the nominal sensitivity may be inaccurate. Meanwhile, perturbation parameters may be coupled together for some optical systems. That means the sensitivity of this kind of systems is singular. As a result, the calculated perturbations are also likely to be inaccurate. To obtain the correct results, more cycles (iterations) are needed. Therefore, the usefulness of STM is limited to some extent. For MFR method [11], it is similar to STM. When merit function is determined, the optimal results can be obtained by several or more iterated STMs. The difference is that sensitivity in STM remains unchanged in the process of reverse-optimization, while sensitivity in MFR method always changes after each cycle. That's because the sensitivity in MFR method is obtained from the optimized system, while the optimized system is always changing before reverse-optimization is finished. MFR method is mostly used in optical design software. So it's easily realized on the ground. But it's hard to be realized on-orbit except that the measurement data can be transferred to the ground continuously. For NAT method [12–16], it is completely different from STM and MFR method. STM and MFR method are numerical, while NAT method is analytical. The inherent analytical characteristic of NAT method can overcome the shortcomings of STM and MFR method. Specially, the computation accuracy of NAT method is much higher than STM. Meantime, it is less sensitive to wave-front measurement errors. Based on these features, NAT method has been widely studied recently. Ju [12] computed astigmatic and trefoil figure errors and misalignments for the on-axis two-mirror telescope using NAT method. Gu [13] aligned an on-axis three-mirror anastigmatic telescope using NAT method. Sebag and Gressler [14] made a Large Synoptic Survey Telescope (LSST) alignment plan based on NAT method. Jiang [15] and Zhang [16] aligned the off-axis telescope based on NAT method. But NAT method was only studied for system recovery before. To compensate the perturbed telescope using NAT method, some new work should be done.

## 2. The principle of system compensation based on nodal aberration theory

Theoretically, the compensated system is still perturbed (That's because the optical system after compensation is not same as the designed). Therefore, nodal aberration theory [12–21], which describes the aberration field of the perturbed system, is also suitable for the compensated system. By introducing aberration field decenter vectors, wave aberration for the perturbed system is expressed as

$$W = \sum_j \sum_p \sum_n \sum_m (W_{klm})_j \left[ (\vec{H} - \vec{\sigma}_j) \cdot (\vec{H} - \vec{\sigma}_j) \right]^p \left[ \vec{\rho} \cdot \vec{\rho} \right]^n \left[ (\vec{H} - \vec{\sigma}_j) \cdot \vec{\rho} \right]^m, \quad k = 2p + m, l = 2n + m \tag{1}$$

where $\vec{H}$ is the normalized field vector, $\vec{\rho}$ is the normalized pupil vector, $\vec{\sigma}_j$ is the introduced aberration field decenter vector of surface $j$, $(W_{klm})_j$ is the corresponding wave aberration coefficient. Note that Eq. (1) only describes the aberration field of on-axis system. For off-axis system, the normalized pupil vector $\vec{\rho}$ in Eq. (1) should be replaced by $(B\vec{\rho} + \vec{h})$. The meanings of $B$ and $\vec{h}$ are referred to Eq. (3) in [16].

In Eq. (1), it can be found that the aberration field of the perturbed system is not linear to aberration field decenter vector. So an idea is presented that the aberration field of the perturbed system can be expanded according to the dependence of aberration field decenter vector. Combined with [22], wave aberration for the perturbed system is modified as

$$W = \sum_i \left[ \sum_k \sum_l \sum_m \sum_q \vec{f}^{\,q}_{klm}(H_x, H_y) \cdot \vec{A}^{q}_{klm}(\vec{\sigma}_x, \vec{\sigma}_y) \right]_i Z_i(\rho, \varphi), \tag{2}$$

Optics EXPRESS

where

$$\sum_k \sum_l \sum_m \sum_q \vec{\mathbf{f}}_{klm}^{q}\left(H_x, H_y\right)\cdot\vec{A}_{klm}^{q}\left(\vec{\sigma}_x, \vec{\sigma}_y\right) = C\left(H_x, H_y\right), \tag{3}$$

$Z(\rho,\varphi)$ is the Zernike term, $C\left(H_x, H_y\right)$ is the corresponding Zernike coefficient, $H_x$ and $H_y$ are the x-component and y-component of $\vec{H}$, $\vec{\sigma}_x$ and $\vec{\sigma}_y$ are the x-component and y-component of $\vec{\sigma}$, $\rho$ and $\varphi$ are the components of $\vec{\rho}$, $q$ denotes the power of aberration field decenter vector. $\vec{A}_{klm}^{q}\left(\vec{\sigma}_x, \vec{\sigma}_y\right)$ is a vector describing the dependence of aberration field decenter vector, $\vec{f}_{klm}^{q}\left(H_x, H_y\right)$ is a vector describing the corresponding dependence of field of view (FOV). Equation (3) can be further expanded, which is followed by

$$\begin{aligned} C\left(H_x, H_y\right) = \vec{f}_{klm}^{0}\left(H_x, H_y\right)\cdot\vec{A}_{klm}^{0}\left(\vec{\sigma}_x, \vec{\sigma}_y\right) + \vec{f}_{klm}^{1}\left(H_x, H_y\right)\cdot\vec{A}_{klm}^{1}\left(\vec{\sigma}_x, \vec{\sigma}_y\right), \\ + \vec{f}_{klm}^{2}\left(H_x, H_y\right)\cdot\vec{A}_{klm}^{2}\left(\vec{\sigma}_x, \vec{\sigma}_y\right) + else \end{aligned} \tag{4}$$

where $\vec{f}_{klm}^{0}\left(H_x, H_y\right)\cdot\vec{A}_{klm}^{0}\left(\vec{\sigma}_x, \vec{\sigma}_y\right)$ denotes the intrinsic property of optical system, which is the residual error of the nominal design. *else* denotes the high-order term of $\vec{\sigma}$ that can be elided, that's because the value of $\vec{\sigma}$ is relatively small. Then the rest denotes the aberration difference before and after system alignment. It should be set to be zero to optimize the perturbed system, which is expressed as

$$\vec{f}_{klm}^{1}\left(H_x, H_y\right)\cdot\vec{A}_{klm}^{1}\left(\vec{\sigma}_x, \vec{\sigma}_y\right) + \vec{f}_{klm}^{2}\left(H_x, H_y\right)\cdot\vec{A}_{klm}^{2}\left(\vec{\sigma}_x, \vec{\sigma}_y\right) = 0, \tag{5}$$

For system recovery, the value of $\vec{\sigma}$ is zero for the recovered system. Equation (5) is absolutely correct. But for system compensation, the value of $\vec{\sigma}$ is not zero for the compensated system. To determine the value of $\vec{\sigma}$, Eq. (5) needs to be solved. Note that $\vec{A}_{klm}^{2}\left(\vec{\sigma}_x, \vec{\sigma}_y\right)$ is not only the function of aberration field decenter vectors, but also the function of figure errors in PM.

For TMA telescopes, all the optical elements (PM, SM and TM) might be perturbed on-orbit. Assuming that only SM is equipped with adjusting mechanism, then aberrations induced from the deformed PM and the misaligned TM need to be compensated by SM to align the perturbed telescope. The deformed PM and the misaligned TM will be discussed to be compensated, respectively, in the following two sections.

## 3. System compensation of the TMA telescope with misaligned TM

### *The basic theory of determining correction values of SM when TM is misaligned*

In this section, the misaligned TM will be firstly discussed. Without figure errors in PM, the higher-order term in Eq. (5) can be further elided. Then Eq. (5) is simplified as

$$\vec{f}_{klm}^{1}\left(H_x, H_y\right)\cdot\vec{A}_{klm}^{1}\left(\vec{\sigma}_x, \vec{\sigma}_y\right) = 0. \tag{6}$$

Considering the dependence of FOVs, Eq. (6) can be further simplified, which is expressed as

$$\vec{A}_{klm}^{1}\left(\vec{\sigma}_x, \vec{\sigma}_y\right) = 0. \tag{7}$$

Note that

Optics EXPRESS

$$\vec{A}_{klm}^{1}\left(\vec{\sigma}_x,\vec{\sigma}_y\right)=\begin{cases}W_{klm,SM}^{(sph)}\vec{\sigma}_{SM,x}^{(sph)}+W_{klm,SM}^{(asph)}\vec{\sigma}_{SM,x}^{(asph)}+W_{klm,TM}^{(sph)}\vec{\sigma}_{TM,x}^{(sph)}+W_{klm,TM}^{(asph)}\vec{\sigma}_{TM,x}^{(asph)}\\ W_{klm,SM}^{(sph)}\vec{\sigma}_{SM,y}^{(sph)}+W_{klm,SM}^{(asph)}\vec{\sigma}_{SM,y}^{(asph)}+W_{klm,TM}^{(sph)}\vec{\sigma}_{TM,y}^{(sph)}+W_{klm,TM}^{(asph)}\vec{\sigma}_{TM,y}^{(asph)}\end{cases}, \quad (8)$$

where $W_{klm,SM}^{sph}$ &$W_{klm,SM}^{asph}$ are the wave aberration coefficients of SM, $W_{klm,TM}^{sph}$ &$W_{klm,TM}^{asph}$ are the wave aberration coefficients of TM, both of them are constant for an optical system. $\vec{\sigma}_{SM,x}^{sph}$ &$\vec{\sigma}_{SM,x}^{asph}$ &$\vec{\sigma}_{SM,y}^{sph}$ &$\vec{\sigma}_{SM,y}^{asph}$ are the components of aberration field decenter vectors of SM, $\vec{\sigma}_{TM,x}^{sph}$ &$\vec{\sigma}_{TM,x}^{asph}$ &$\vec{\sigma}_{TM,y}^{sph}$ &$\vec{\sigma}_{TM,y}^{asph}$ are the components of aberration field decenter vectors of TM, *sph* and *asph* denote the spherical and aspherical contributions, respectively.

On the premise that the misalignments of TM are known, the aberration field decenter vectors of TM can be accurately expressed based on NAT. The expressions are followed by

$$\begin{cases}\vec{\sigma}_{TM,x}^{sph}=\dfrac{F_x+C\cdot\vec{\sigma}_{SM,x}^{sph}}{Q}\\ \vec{\sigma}_{TM,y}^{sph}=\dfrac{F_y+C\cdot\vec{\sigma}_{SM,y}^{sph}}{Q}\end{cases}\quad\begin{cases}\vec{\sigma}_{TM,x}^{asph}=\dfrac{E_x+D\cdot\vec{\sigma}_{SM,x}^{sph}}{R}\\ \vec{\sigma}_{TM,y}^{asph}=\dfrac{E_y+D\cdot\vec{\sigma}_{SM,y}^{sph}}{R}\end{cases}, \quad (9)$$

where

$$\begin{cases}Q=\left[c_{TM}\left(d_2-d_1\right)+2c_{SM}\left(c_{TM}d_1d_2+d_1\right)+1\right]\bar{u}_{PM}\\ R=\left[d_2+d_1\left(2c_{SM}d_2-1\right)\right]\bar{u}_{PM}\\ C=2\left(1+c_{TM}d_2\right)\left(1+c_{SM}d_1\right)\bar{u}_{PM}\\ D=2d_2\left(1+c_{SM}d_1\right)\bar{u}_{PM}\end{cases}, \quad (10)$$

$$\begin{cases}E_x=XDE_{TM}\\ F_x=c_{TM}XDE_{TM}-BDE_{TM}\\ E_y=YDE_{TM}\\ F_y=c_{TM}YDE_{TM}+ADE_{TM}\end{cases}. \quad (11)$$

Here $\bar{u}_{PM}$ is the paraxial chief ray incident angle at PM, $d_1$ and $d_2$ are the thickness of PM and SM, $c_{SM}$ and $c_{TM}$ are the curvature of SM and TM, they are all constant. $XDE_{TM}$ &$YDE_{TM}$ &$ADE_{TM}$ &$BDE_{TM}$ are the misalignments of TM. Then Eq. (7) can be expanded as

$$\begin{cases}\left(W_{klm,SM}^{(sph)}+\dfrac{C}{Q}W_{klm,TM}^{(sph)}+\dfrac{D}{R}W_{klm,TM}^{(asph)}\right)\vec{\sigma}_{SM,x}^{(sph)}+W_{klm,SM}^{(asph)}\vec{\sigma}_{SM,x}^{(asph)}+\dfrac{F_x}{Q}W_{klm,TM}^{(sph)}+\dfrac{E_x}{R}W_{klm,TM}^{(asph)}=0\\ \left(W_{klm,SM}^{(sph)}+\dfrac{C}{Q}W_{klm,TM}^{(sph)}+\dfrac{D}{R}W_{klm,TM}^{(asph)}\right)\vec{\sigma}_{SM,y}^{(sph)}+W_{klm,SM}^{(asph)}\vec{\sigma}_{SM,y}^{(asph)}+\dfrac{F_y}{Q}W_{klm,TM}^{(sph)}+\dfrac{E_y}{R}W_{klm,TM}^{(asph)}=0\end{cases}, \quad (12)$$

As is known, third-order aberrations are dominating for the perturbed telescope, especially third-order astigmatism and third-order coma. To align the perturbed telescope, third-order aberrations must be corrected after compensation. That means third-order astigmatism ($W_{222}$) and third-order coma ($W_{131}$) are considered in Eq. (12). Then Eq. (12) can be expressed by two matrices, which are followed by

Optics EXPRESS

$$\begin{bmatrix} W_{222,SM}^{(sph)}+\frac{C}{Q}W_{222,TM}^{(sph)}+\frac{D}{R}W_{222,TM}^{(asph)} & W_{222,SM}^{(asph)} \\ W_{131,SM}^{(sph)}+\frac{C}{Q}W_{131,TM}^{(sph)}+\frac{D}{R}W_{131,TM}^{(asph)} & W_{131,SM}^{(asph)} \end{bmatrix} \begin{bmatrix} \vec{\sigma}_{SM,x}^{(sph)} \\ \vec{\sigma}_{SM,x}^{(asph)} \end{bmatrix} = -\begin{bmatrix} \frac{F_x}{Q}W_{222,TM}^{(sph)}+\frac{E_x}{R}W_{222,TM}^{(asph)} \\ \frac{F_x}{Q}W_{131,TM}^{(sph)}+\frac{E_x}{R}W_{131,TM}^{(asph)} \end{bmatrix}, \quad (13)$$

$$\begin{bmatrix} W_{222,SM}^{(sph)}+\frac{C}{Q}W_{222,TM}^{(sph)}+\frac{D}{R}W_{222,TM}^{(asph)} & W_{222,SM}^{(asph)} \\ W_{131,SM}^{(sph)}+\frac{C}{Q}W_{131,TM}^{(sph)}+\frac{D}{R}W_{131,TM}^{(asph)} & W_{131,SM}^{(asph)} \end{bmatrix} \begin{bmatrix} \vec{\sigma}_{SM,y}^{(sph)} \\ \vec{\sigma}_{SM,y}^{(asph)} \end{bmatrix} = -\begin{bmatrix} \frac{F_y}{Q}W_{222,TM}^{(sph)}+\frac{E_y}{R}W_{222,TM}^{(asph)} \\ \frac{F_y}{Q}W_{131,TM}^{(sph)}+\frac{E_y}{R}W_{131,TM}^{(asph)} \end{bmatrix}. \quad (14)$$

By solving Eqs. (13) and (14), the aberration field vectors of SM can be determined. Then the correction values of SM ( $XDE_{SM}$ & $YDE_{SM}$ & $ADE_{SM}$ & $BDE_{SM}$ ) can be determined based on the following equation.

$$\begin{cases} XDE_{SM} = -\bar{u}_{PM} d_1 \vec{\sigma}_{SM,x}^{(asph)} \\ YDE_{SM} = -\bar{u}_{PM} d_1 \vec{\sigma}_{SM,y}^{(asph)} \\ ADE_{SM} = -\bar{u}_{PM}\left(1+c_{SM} d_1\right)\vec{\sigma}_{SM,y}^{(sph)} - c_{SM} YDE_{SM} \\ BDE_{SM} = \bar{u}_{PM}\left(1+c_{SM} d_1\right)\vec{\sigma}_{SM,x}^{(sph)} + c_{SM} YDE_{SM} \end{cases}. \quad (15)$$

*Examples of compensating the misaligned TM for both on-axis and off-axis TMA telescopes*

As described above, the correction values of SM used for compensating the misaligned TM can be accurately determined based on Eqs. (13)-(15). In this subsection, an on-axis TMA telescope and an off-axis TMA telescope are selected to validate this compensation principle. The on-axis TMA telescope is referred to [16]. It is a 6.6m F/14 telescope with a 0.3° × 0.15° FOV and a 0.18° field offset. The off-axis TMA telescope is referred to [16]. It is a 600mm F/10 telescope with a 2.75° × 0.25° FOV and a –0.3° field offset. Their aperture stops are both located at PM. The optical layout of them is shown in Fig. 1. The optical prescriptions of them are listed in Table 1 and Table 2, respectively. The wave aberration coefficients of SM and TM of them are listed in Table 3 and Table 4, respectively.

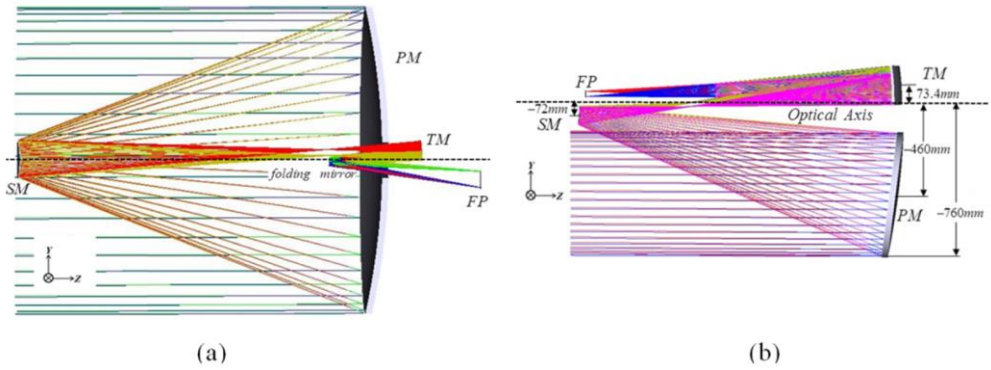


(a) (b)

Fig. 1. The optical layout of the selected TMA telescopes (a) the on-axis TMA telescope (b) the off-axis telescope.

Optics EXPRESS

**Table 1. Optical prescription of the selected on-axis TMA telescope**

| Surface | Type | Conic constant | Radius(mm) | Thickness(mm) |
|---|---|---|---|---|
| PM(stop) | Conic | –0.9948 | –16287.099 | –7170 |
| SM | Conic | –1.8351 | –2317.426 | 7965 |
| TM | Conic | –0.7202 | –2702.327 | –1845 |
| Folding mirror | | | Infinity | 3006.205 |
| Image Plane | | | Infinity | |

**Table 2. Optical prescription of the selected off-axis TMA telescope**

| Surface | Type | Conic constant | Radius(mm) | Thickness(mm) |
|---|---|---|---|---|
| PM(stop) | Conic | - - | –3600.41 | –1551.777 |
| SM | Conic | - - | –910.903 | 1558.7 |
| TM | Conic | - - | –1219.431 | –1533.359 |
| Image Plane | | | Infinity | |

**Table 3. Wave aberration coefficients of SM and TM for the selected on-axis TMA telescope**

| $W_{222,SM}^{(sph)}/\lambda$ | $W_{222,SM}^{(asph)}/\lambda$ | $W_{222,TM}^{(sph)}/\lambda$ | $W_{222,TM}^{(asph)}/\lambda$ | $W_{131,SM}^{(sph)}/\lambda$ | $W_{131,SM}^{(asph)}/\lambda$ | $W_{131,TM}^{(sph)}/\lambda$ | $W_{131,TM}^{(asph)}/\lambda$ |
|---|---|---|---|---|---|---|---|
| –2.9114 | 3.0514 | 3.9028 | –5.7613 | 31.9156 | 32.0651 | 0.8899 | 2.0713 |

Note that the wavelength in the selected on-axis TMA telescope is 10600nm.

**Table 4. Wave aberration coefficients of SM and TM for the selected off-axis TMA telescope**

| $W_{222,SM}^{(sph)}/\lambda$ | $W_{222,SM}^{(asph)}/\lambda$ | $W_{222,TM}^{(sph)}/\lambda$ | $W_{222,TM}^{(asph)}/\lambda$ | $W_{131,SM}^{(sph)}/\lambda$ | $W_{131,SM}^{(asph)}/\lambda$ | $W_{131,TM}^{(sph)}/\lambda$ | $W_{131,TM}^{(asph)}/\lambda$ |
|---|---|---|---|---|---|---|---|
| –87.0055 | 166.7856 | 190.4173 | –424.6751 | 390.3568 | 445.3313 | 98.1885 | 386.9590 |

Note that the wavelength in the selected off-axis TMA telescope is 650nm.

In the process of system compensation, only astigmatic field ($W_{222}$) and comatic field ($W_{131}$) are considered above. Their corresponding Fringe Zernike coefficients are $C_{5/6}$ (astigmatism) and $C_{7/8}$ (coma), respectively. By calculating these coefficients of each FOV, astigmatic field and comatic field can be characterized through Full-Field-Display (FFD). As shown in Fig. 2 and Fig. 3, the nominal astigmatic field and comatic field for on-axis TMA telescope and off-axis TMA telescope are visualized.

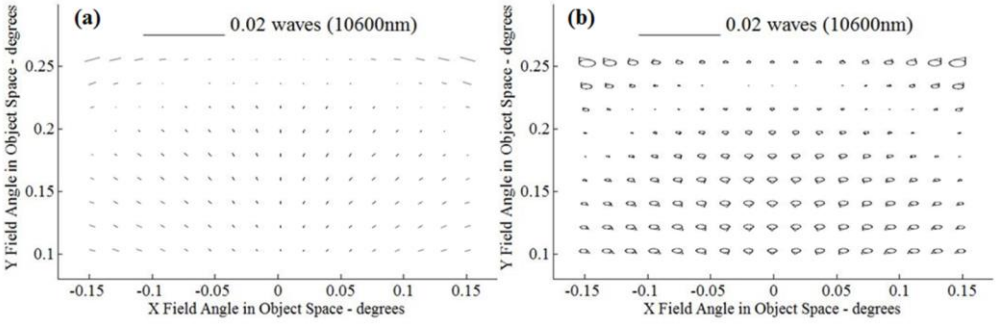


Fig. 2. FFDs of the Fringe Zernike coefficients for the nominal on-axis TMA telescope (a) $C_{5/6}$ (astigmatism) (average value = 0.0018λ) (b) $C_{7/8}$ (coma) (average value = 0.0017λ).

Optics EXPRESS

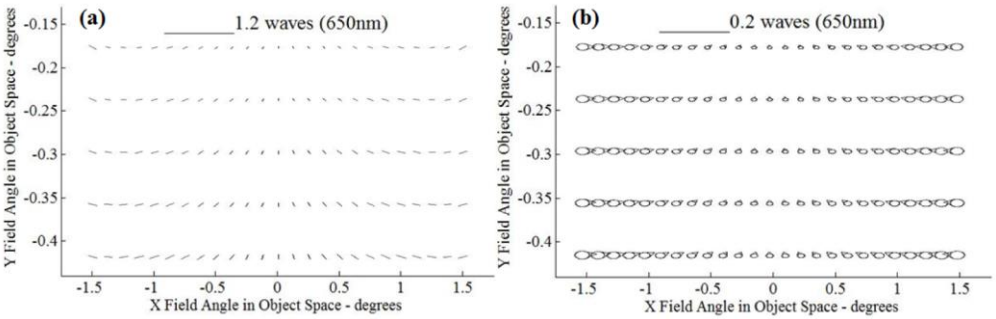


Fig. 3. FFDs of the Fringe Zernike coefficients for the nominal off-axis TMA telescope (a) $C_{5/6}$ (astigmatism) (average value = 0.1183λ) (b) $C_{7/8}$ (coma) (average value = 0.0327λ).

In active optics, the values of misalignments are very small. Generally, lateral misalignments (*XDE*&*YDE*) are on the level of micrometers, and angular misalignments (*ADE*&*BDE*) are on the level of arccseconds. In this subsection, the introduced misalignments of TM are listed in Table 5. The values are same for on-axis TMA telescope and off-axis TMA telescope. Based on the compensation principle, the correction values of SM can be calculated. They are listed in Table 6. Meantime, the astigmatic field and comatic field after misalignment and compensation for the two TMA telescopes are characterized and visualized in Figs. 4-7.

**Table 5. The introduced misalignments of TM for on-axis TMA telescope and off-axis TMA telescope**

| $XDE_{TM}$ / mm | $YDE_{TM}$ / mm | $ADE_{TM}$ / ° | $BDE_{TM}$ / ° |
|---|---|---|---|
| 0.06 | –0.04 | –0.005 | 0.005 |

**Table 6. The calculated correction values of SM for adjusting the misaligned TM of on-axis TMA telescope and off-axis TMA telescope**

| | $XDE_{SM}$ / mm | $YDE_{SM}$ / mm | $ADE_{SM}$ / ° | $BDE_{SM}$ / ° |
|---|---|---|---|---|
| On-axis TMA telescope | –0.0201 | –0.0196 | –0.001057 | 0.001047 |
| Off-axis TMA telescope | –0.0461 | –0.0259 | –0.002948 | 0.003842 |

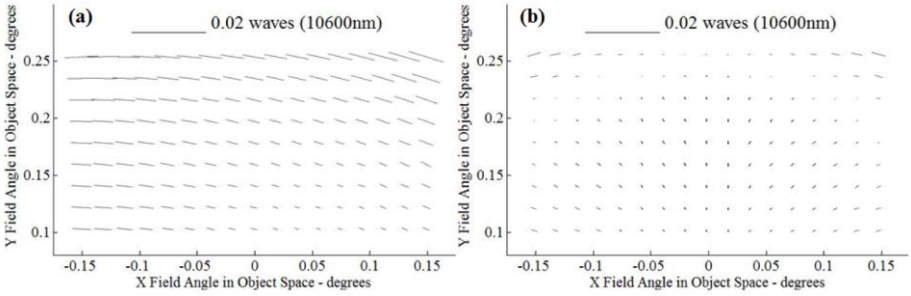


Fig. 4. FFDs of the Fringe Zernike coefficients $C_{5/6}$ for the on-axis TMA telescope after misalignment and compensation (a) misalignment (average value = 0.0034λ) (b) compensation (average value = 0.0018λ).

Optics EXPRESS

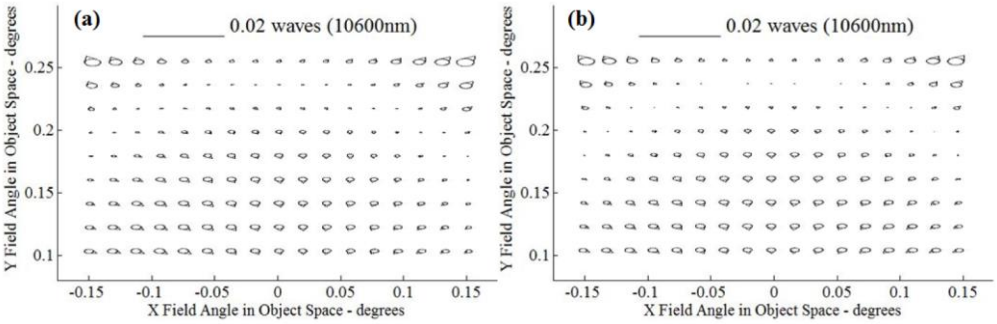


Fig. 5. FFDs of the Fringe Zernike coefficients $C_{7/8}$ for the on-axis TMA telescope after misalignment and compensation (a) misalignment (average value = 0.0018λ) (b) compensation (average value = 0.0017λ).

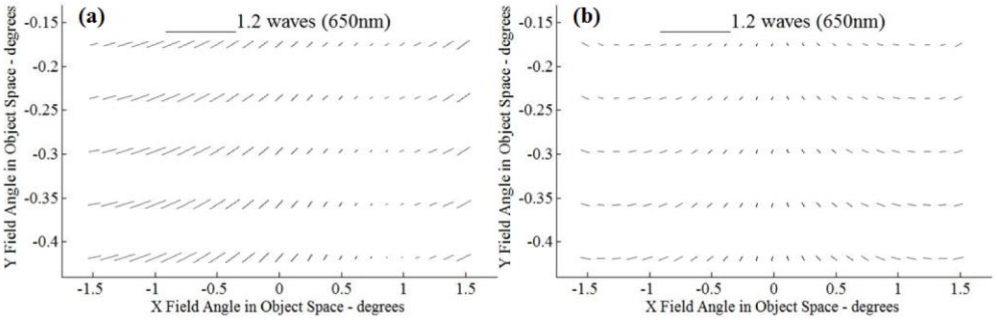


Fig. 6. FFDs of the Fringe Zernike coefficients $C_{5/6}$ for the off-axis TMA telescope after misalignment and compensation (a) misalignment (average value = 0.1290λ) (b) compensation (average value = 0.1183λ).

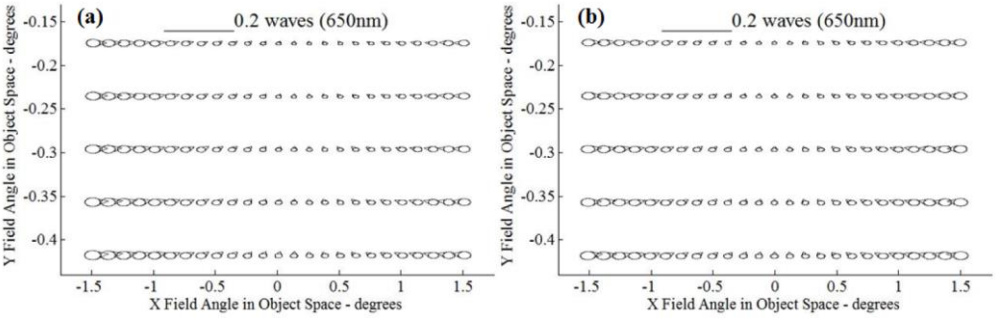


Fig. 7. FFDs of the Fringe Zernike coefficients $C_{7/8}$ for the off-axis TMA telescope after misalignment and compensation (a) misalignment (average value = 0.0332λ) (b) compensation (average value = 0.0331λ).

From Figs. 4-7, it can be found that more astigmatic aberrations but less comatic aberrations are induced from TM misalignment. Compared Fig. 4-5 with Fig. 2, it is shown that the astigmatic aberrations and comatic aberrations induced from the misaligned TM can be accurately compensated by adjusting SM for the on-axis TMA telescope. The same conclusion can also be made for the off-axis TMA telescope by comparing Figs. 6 and 7 with Fig. 3.

Optics EXPRESS

## 4. System compensation of the TMA telescope with deformed PM

### *The basic theory of determining correction values of SM when PM is deformed*

In this section, the deformed PM will be discussed. For primary mirror (the aperture stop for the selected TMA telescopes), the common figure errors are astigmatism induced from mounting. To compensate the astigmatic figure errors in PM, Eq. (5) also needs to be established.

In Eq. (5), there exist linear term and quadratic term. The linear term is only the function of aberration field decenter vectors. While the quadratic term is not only the function of aberration field decenter vectors, but also the function of astigmatic figure errors in PM (referred to [23]). In the process of TM compensation, only the linear term is considered, the quadratic term can be ignored as described in section 3. But for the compensation of the deformed PM, both linear term and quadratic term need to be considered.

Similar to the compensation of the misaligned TM, only third order astigmatism and third order coma will be corrected in the process of PM compensation. Considering the contributions from astigmatic figure errors in PM, Eq. (5) can be expressed by two equations, which are followed by

$$\vec{\boldsymbol{f}}^{1}_{131}\left(H_x,H_y\right)\cdot\vec{\boldsymbol{A}}^{1}_{131}\left(\vec{\sigma}_x,\vec{\sigma}_y\right)=0, \tag{16}$$

$$\vec{\boldsymbol{f}}^{1}_{222}\left(H_x,H_y\right)\cdot\vec{\boldsymbol{A}}^{1}_{222}\left(\vec{\sigma}_x,\vec{\sigma}_y\right)+\vec{\boldsymbol{f}}^{2}_{222}\left(H_x,H_y\right)\cdot\vec{\boldsymbol{A}}^{2}_{222}\left(\vec{\sigma}_x,\vec{\sigma}_y\right)=0, \tag{17}$$

where $\vec{\boldsymbol{f}}^{1}_{222}\left(H_x,H_y\right)=B^2\begin{bmatrix}-2H_x & 2H_y\\ -2H_y & -2H_x\end{bmatrix}$, $\vec{\boldsymbol{f}}^{2}_{222}\left(H_x,H_y\right)=B^2\begin{bmatrix}1 & 0\\ 0 & 1\end{bmatrix}$, $\vec{\boldsymbol{A}}^{2}_{222}\left(\vec{\sigma}_x,\vec{\sigma}_y\right)\approx\frac{1}{B^2}\vec{\boldsymbol{A}}^{2}_{222,Fig}=\frac{-4}{B^2}\begin{bmatrix}C^{PM}_{5,Fig}\\ C^{PM}_{6,Fig}\end{bmatrix}$, $B$ is the scaling factor for off-axis system, its value is 1 for on-axis system, $C^{PM}_{5,Fig}$ and $C^{PM}_{6,Fig}$ denote the astigmatic figure errors in PM. Equation (16) is just a special case of Eq. (6). It can be simplified to Eq. (7), where *klm* = 131. That means the x-component and y-component of $\vec{\boldsymbol{A}}^{1}_{131}\left(\vec{\sigma}_x,\vec{\sigma}_y\right)$ are 0. Equation (17) is much more complicated. Considering the dependence of FOV, it can be expanded by

$$\begin{bmatrix}-H_x & H_y\\ -H_y & -H_x\end{bmatrix}\begin{bmatrix}\vec{\boldsymbol{A}}^{1}_{222,x}\left(\vec{\sigma}_x,\vec{\sigma}_y\right)\\ \vec{\boldsymbol{A}}^{1}_{222,y}\left(\vec{\sigma}_x,\vec{\sigma}_y\right)\end{bmatrix}=\frac{2}{B^2}\begin{bmatrix}C^{PM}_{5,Fig}\\ C^{PM}_{6,Fig}\end{bmatrix}. \tag{18}$$

Based on Eq. (18), the x-component and y-component of $\vec{\boldsymbol{A}}^{1}_{222}\left(\vec{\sigma}_x,\vec{\sigma}_y\right)$ can be determined. Note that the solution of Eq. (18) is least squared. By combining $\vec{\boldsymbol{A}}^{1}_{131}\left(\vec{\sigma}_x,\vec{\sigma}_y\right)$ and $\vec{\boldsymbol{A}}^{1}_{222}\left(\vec{\sigma}_x,\vec{\sigma}_y\right)$, the aberration field decenter vectors of SM can be determined referred to Eqs. (8)-(12). Note that TM is not misaligned in this section. The values of all the quantities in Eq. (11) are equal 0. On the premise that the astigmatic figure errors of PM are known, the aberration field decenter vectors of SM used for compensating the deformed PM can be determined by

$$\begin{bmatrix}W^{(sph)}_{222,SM}+\frac{C}{Q}W^{(sph)}_{222,TM}+\frac{D}{R}W^{(asph)}_{222,TM} & W^{(asph)}_{222,SM}\\ W^{(sph)}_{131,SM}+\frac{C}{Q}W^{(sph)}_{131,TM}+\frac{D}{R}W^{(asph)}_{131,TM} & W^{(asph)}_{131,SM}\end{bmatrix}\begin{bmatrix}\vec{\sigma}^{(sph)}_{SM,x}\\ \vec{\sigma}^{(asph)}_{SM,x}\end{bmatrix}=\begin{bmatrix}\vec{\boldsymbol{A}}^{1}_{222,x}\left(\vec{\sigma}_x,\vec{\sigma}_y\right)\\ 0\end{bmatrix}, \tag{19}$$

Optics EXPRESS

$$\begin{bmatrix} W_{222,SM}^{(sph)}+\frac{C}{Q}W_{222,TM}^{(sph)}+\frac{D}{R}W_{222,TM}^{(asph)} & W_{222,SM}^{(asph)} \\ W_{131,SM}^{(sph)}+\frac{C}{Q}W_{131,TM}^{(sph)}+\frac{D}{R}W_{131,TM}^{(asph)} & W_{131,SM}^{(asph)} \end{bmatrix} \begin{bmatrix} \vec{\sigma}_{SM,y}^{(sph)} \\ \vec{\sigma}_{SM,y}^{(asph)} \end{bmatrix} = \begin{bmatrix} \vec{A}_{222,y}^{1}\left(\vec{\sigma}_x,\vec{\sigma}_y\right) \\ 0 \end{bmatrix}. \quad (20)$$

Then the correction values of SM ( $XDE_{SM}$ & $YDE_{SM}$ & $ADE_{SM}$ & $BDE_{SM}$ ) can be determined based on Eq. (15).

### *Examples of compensating the deformed PM for both on-axis and off-axis TMA telescopes*

Based on the derived theory above, the correction values of SM for compensating the deformed PM can be determined. To validate the compensation theory, the same on-axis TMA telescope and off-axis TMA telescope mentioned in section 3 are simulated. The introduced astigmatic figure errors of PM are listed in Table 7, the values of which are same for on-axis TMA telescope and off-axis TMA telescope. The calculated correction values of SM are listed in Table 8. Meantime, the astigmatic field after deformation and compensation for the two TMA telescopes is characterized and visualized in Fig. 8 and Fig. 9. Note that the comatic field is not characterized here. That's because the astigmatic figure errors of PM do not have contributions to comatic field. And the comatic field has a little or even no changes after compensation.

From Fig. 8, it can be seen that the figure errors in PM have the same aberration contributions to each FOV for the on-axis TMA telescope. And the astigmatic field has been corrected to some extent after compensation. But the astigmatic field is not fully corrected compared to Fig. 2(a). That may be because the values of $\vec{A}_{222}^{1}\left(\vec{\sigma}_x,\vec{\sigma}_y\right)$ is solved based on least square method. As a result, only a portion of FOVs can be corrected well. The same conclusion can also be made for the off-axis TMA telescope from Fig. 9. Therefore, some other means are studied to completely correct the constant aberration induced from PM, like placing the deformation mirrors in the location of the image of pupil.

**Table 7. The introduced astigmatic figure errors of PM for on-axis TMA telescope and off-axis TMA telescope**

| $C_{5,Fig}^{PM}/\lambda$ | $C_{6,Fig}^{PM}/\lambda$ |
|---|---|
| 0.05 | –0.05 |

**Table 8. The calculated correction values of SM for adjusting the deformed PM of on-axis TMA telescope and off-axis TMA telescope**

| | $XDE_{SM}/mm$ | $YDE_{SM}/mm$ | $ADE_{SM}/°$ | $BDE_{SM}/°$ |
|---|---|---|---|---|
| On-axis TMA telescope | 0.428 | 0.428 | 0.024 | –0.024 |
| Off-axis TMA telescope | –0.0515 | –0.0515 | –0.001285 | 0.001285 |

Optics EXPRESS

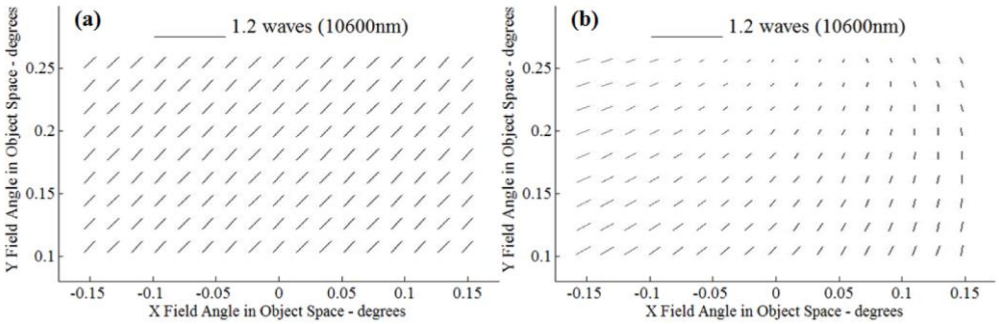


Fig. 8. FFDs of the astigmatic aberration field ( $C_{5/6}$ ) for the on-axis TMA telescope after deformation and compensation (a) deformation (average value = 0.1341λ) (b) compensation (average value = 0.0707λ).

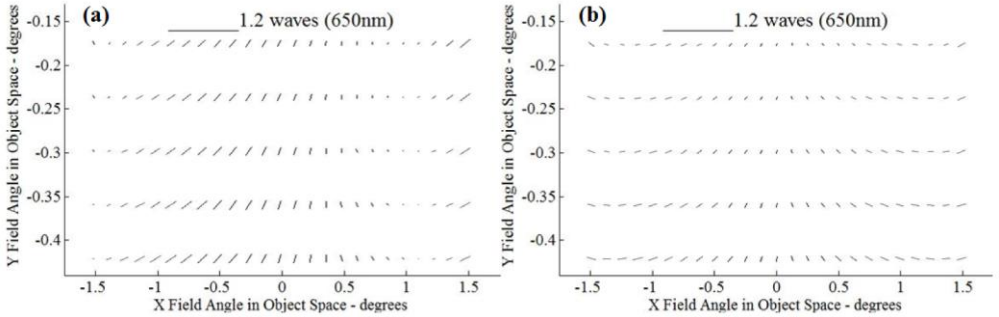


Fig. 9. FFDs of the astigmatic aberration field ( $C_{5/6}$ ) for the off-axis TMA telescope after deformation and compensation (a) deformation (average value = 0.1602λ) (b) compensation (average value = 0.1175λ).

## 5. Comparison of NAT method and MFR method

For system recovery, the calculated correction values can be evaluated by comparing them with the introduced directly. But for system compensation, they can't be compared directly (That's because the introduced perturbations are about PM and TM, while the calculated compensations are about SM). To evaluate the calculated correction values based on the proposed NAT method here, the referred values (standard values) should be firstly determined. As a matter of fact, they can be obtained by merit function regression (MFR) method, which can be realized in optical software.

For MFR method, the merit function (*MF*) should be firstly defined. Generally, it is defined as

$$MF^2 = \frac{\sum_i W_i \left(V_i - T_i\right)^2}{\sum_i W_i}, \tag{21}$$

where $W_i$ is the weight, $V_i$ is the value after regression, $T_i$ is the target value, $i$ indicates the aberration number needed to be regressed. To compensate the perturbed optical system, the value of *MF* should be minimized. In this paper, only third order astigmatic field and third order comatic field are considered. Hence third order astigmatic and third order coma for different FOVs are chosen to Eq. (21) in the process of merit function regression.

Here the same on-axis TMA telescope and off-axis TMA telescope in section 3 are simulated. And the misalignments of TM and the deformations of PM remain unchanged. By

Optics EXPRESS

MFR method, the correction values of SM for compensating PM or TM of these two telescopes can be calculated. Then the referred values are determined. At the same time, the relative errors of the correction values based on NAT method and MFR method can also be calculated. These results have been listed in Table 9 and Table 10.

From Table 9 and Table 10, it can be found that the calculated correction values based on NAT method are very close to the correction values resulting from MFR method (Note that the relative errors of off-axis TMA telescope are larger. That's may be because the off-axis TMA telescope is not diffraction-limited. The perturbed system may be further optimized by MFR method. While NAT method doesn't has the capability of optimization. As a result, the relative errors between these two methods are slightly large. The on-axis TMA telescope is more convictive). It indicates that the calculated correction values in section 3 and section 4 are correct. Therefore, the principle of system compensation developed in this paper is well demonstrated.

**Table 9. The calculated correction values of SM for the misaligned TM of on-axis TMA telescope and off-axis TMA telescope based on NAT method and MFR method and their relative errors**

| | | $XDE_{SM}$ / mm | $YDE_{SM}$ / mm | $ADE_{SM}$ / ° | $BDE_{SM}$ / ° |
|---|---|---|---|---|---|
| On-axis TMA telescope | NAT method | –0.0201 | –0.0196 | –0.001057 | 0.001047 |
| | MFR method | –0.0203 | –0.0199 | –0.001069 | 0.001057 |
| | Relative error | **0.99%** | **1.51%** | **1.12%** | **0.95%** |
| Off-axis TMA telescope | NAT method | –0.0461 | –0.0259 | –0.002948 | 0.003842 |
| | MFR method | –0.0477 | –0.0277 | –0.003034 | 0.003887 |
| | Relative error | **3.35%** | **6.50%** | **2.83%** | **1.16%** |

**Table 10. The calculated correction values of SM for the deformed PM of on-axis TMA telescope and off-axis TMA telescope based on NAT method and MFR method and their relative errors**

| | | $XDE_{SM}$ / mm | $YDE_{SM}$ / mm | $ADE_{SM}$ / ° | $BDE_{SM}$ / ° |
|---|---|---|---|---|---|
| On-axis TMA telescope | NAT method | 0.428 | 0.428 | 0.024 | –0.024 |
| | MFR method | 0.4248 | 0.4252 | 0.0233 | –0.0232 |
| | Relative error | **0.75%** | **0.66%** | **3.00%** | **3.45%** |
| Off-axis TMA telescope | NAT method | –0.0515 | –0.0515 | –0.001285 | 0.001285 |
| | MFR method | –0.0520 | –0.0542 | –0.001382 | 0.001304 |
| | Relative error | **0.96%** | **4.98%** | **7.02%** | **1.46%** |

## 6. Comparison of NAT method and STM

As described in the introduction, MFR method is limited to some extent in the practical application. In the engineering, sensitivity table method (STM) is more usually used. To demonstrate the application of the proposed NAT method here, it should be compared to STM.

In this section, eight Monte-Carlo simulations that correspond to four different cases for on-axis TMA telescope and off-axis TMA telescope, respectively, as shown in Table 11, will be performed to compare NAT method and STM. Note that only TM is compensated here. That's because PM can be partially compensated as concluded in section 4. The aberration

Optics EXPRESS

field after compensation can't be compared with the nominal design. However, TM can be completely compensated as concluded in section 3. It can be used to be compared with the nominal design. In Case 1, Case 2 and Case 3, the perturbation ranges increase step by step, but without any measurement error. In Case 4, the perturbation ranges are the same as Case 2, but with 2% measurement error.

**Table 11. The four different cases considered in the Monte-Carlo simulations**

| | $XDE_{TM}, YDE_{TM}$ | $ADE_{TM}, BDE_{TM}$ |
|---|---|---|
| Case 1 | [-0.05,0.05] | [-0.005,0.005] |
| Case 2 | [-0.1,0.1] | [-0.01,0.01] |
| Case 3 | [-0.5,0.5] | [-0.05,0.05] |
| Case 4 | [-0.1,0.1] | [-0.01,0.01] |
| | With 2% measurement error | |

In each case, 100 pairs of random perturbations following a standard uniform distribution are generated. For each perturbed state, the correction values can be calculated based on NAT method and STM, respectively. Then the calculated correction values are used to compensate the perturbed system. Here the averaged values of C5/C6 after misalignment and compensation are compared. For on-axis TMA telescope, the averaged value of C5/C6 is calculated with 17 × 9 equally spaced field point in 0.3° × 0.15°. For off-axis TMA telescope, the averaged value of C5/C6 is calculated with 25 × 5 equally spaced field point in 3° × 0. 3°.

Compared Fig. 10 with Fig. 11, we can see that the misaligned on-axis systems in any case (even if there exist measurement errors) can always be compensated to the nominal design based on NAT method. But for STM, the misaligned systems can only be compensated in small perturbation ranges and without any measurement errors (Case 1). If the perturbation ranges are larger (Case 2 and Case 3) or the measured wave-front coefficients are not very accurate (Case 4), the alignment process based on STM becomes unsuccessful at some misaligned states. It can be concluded that the computation accuracy of correction values based on NAT method is relatively higher than that based on STM for on-axis TMA telescope. Meanwhile, the same conclusion can be made for off-axis TMA telescope by comparing Fig. 12 with Fig. 13.

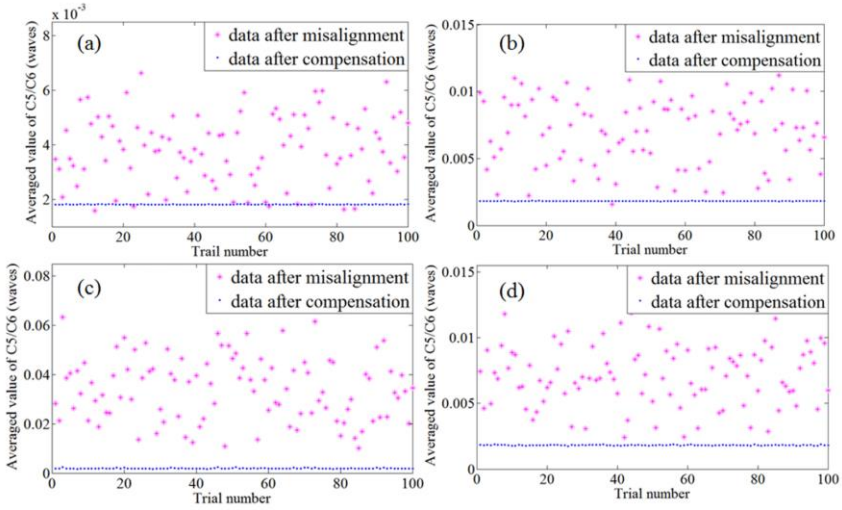


Fig. 10. Averaged values of astigmatism ( $C_{5/6}$ ) for the on-axis TMA telescope after misalignment and compensation for different cases based on NAT method. (a) Case 1 (b) Case 2 (c) Case 3 (d) Case 4. Note that the pink spots represent the averaged values of astigmatism after misalignment. The blue spots represent the averaged values of astigmatism after compensation.

Optics EXPRESS

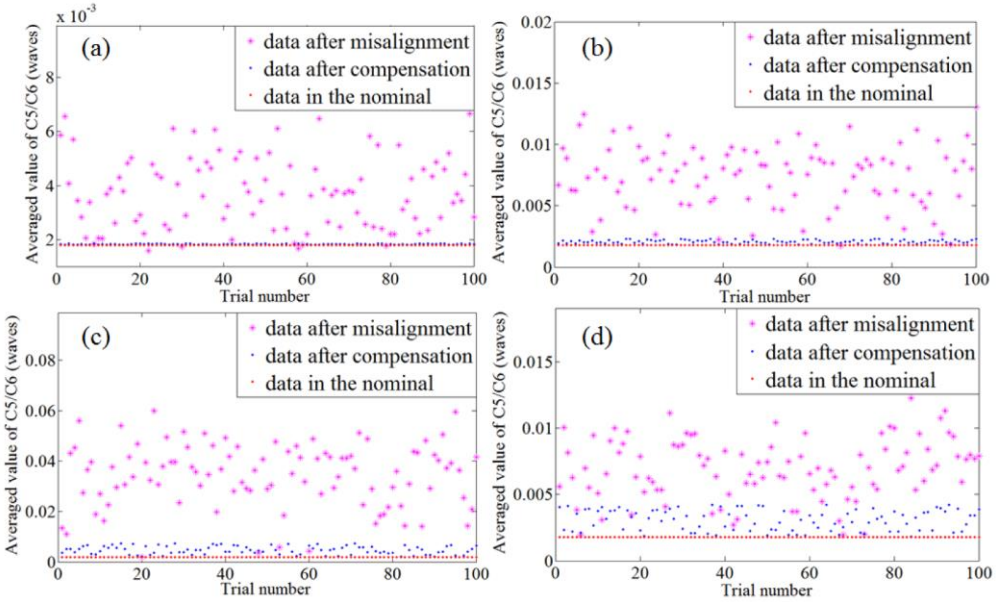


Fig. 11. Averaged values of astigmatism ( $C_{5/6}$ ) for the on-axis TMA telescope after misalignment and compensation for different cases based on STM method. (a) Case 1 (b) Case 2 (c) Case 3 (d) Case 4. Note that the pink spots represent the averaged values of astigmatism after misalignment. The blue spots represent the averaged values of astigmatism after compensation. The red spots represent the averaged values of astigmatism in the nominal design.

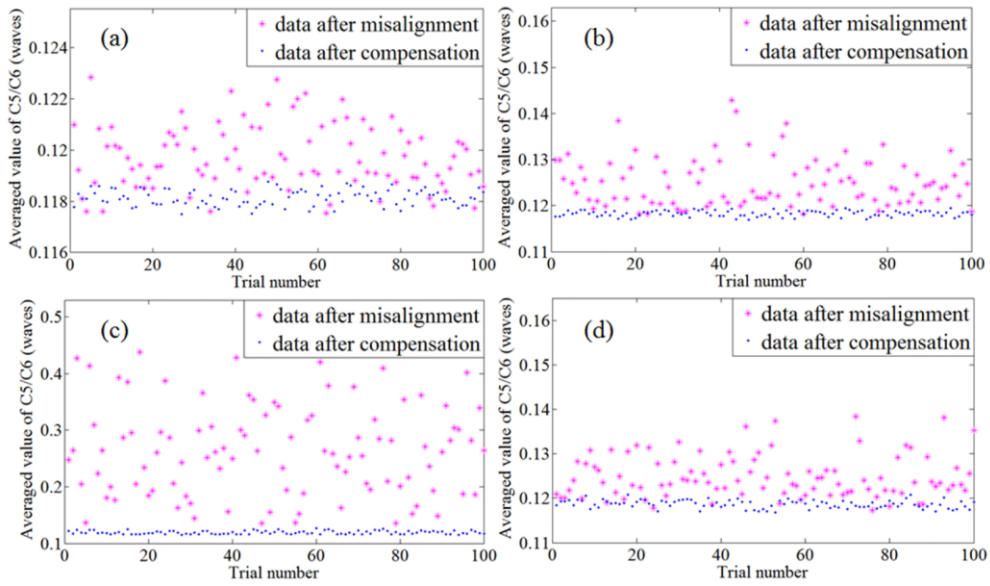


Fig. 12. Averaged values of astigmatism ( $C_{5/6}$ ) for the off-axis TMA telescope after misalignment and compensation for different cases based on NAT method. (a) Case 1 (b) Case 2 (c) Case 3 (d) Case 4. Note that the pink spots represent the averaged values of astigmatism after misalignment. The blue spots represent the averaged values of astigmatism after compensation.

Optics EXPRESS

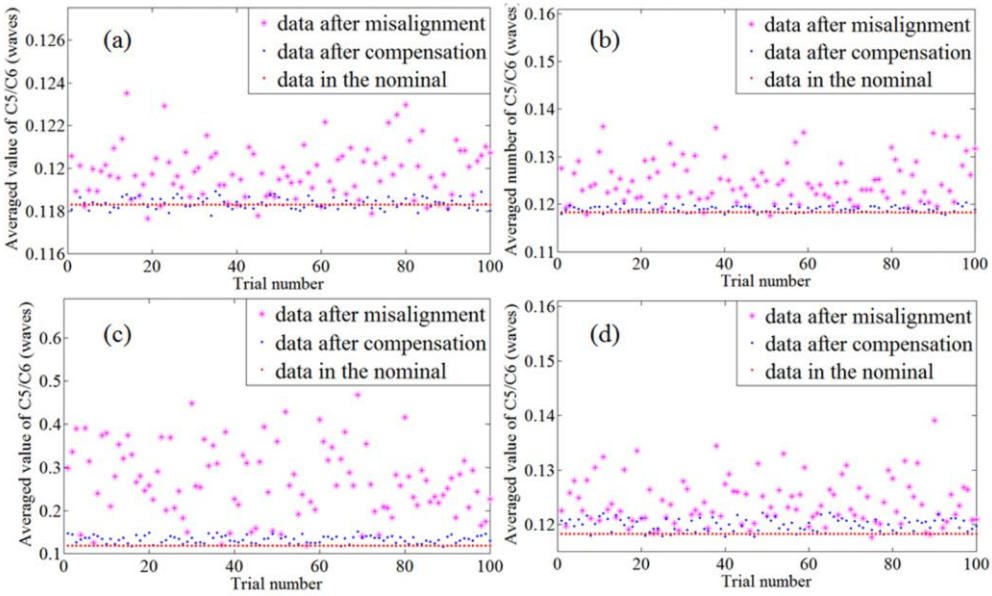


Fig. 13. Averaged values of astigmatism ( $C_{5/6}$ ) for the off-axis TMA telescope after misalignment and compensation for different cases based on STM method. (a) Case 1 (b) Case 2 (c) Case 3 (d) Case 4. Note that the pink spots represent the averaged values of astigmatism after misalignment. The blue spots represent the averaged values of astigmatism after compensation. The red spots represent the averaged values of astigmatism in the nominal design.

Therefore, NAT method is more applicable for the optical compensation of the perturbed TMA telescope, either on-axis or off-axis. Compared with NAT method, NAT method is a better choice.

## 7. Conclusion

In this paper, wave aberration is expanded to the product of the dependence of field of view and the dependence of aberration field decenter vector. Then the principle of system compensation is presented considering the order of aberration field decenter vector in active optics. Next, the misaligned TM and deformed PM of an on-axis TMA telescope and an off-axis TMA telescope are studied to be compensated by SM according to the derived theory of system compensation (NAT method). In the end, NAT method is compared with MFR method to validate the correctness of optical compensation based on NAT. Meanwhile, NAT method is compared with STM to demonstrate its application by Monte-Carlo simulations.

By expansion, it can be found that wave aberration is only related with FOVs and aberration field decenter vectors. It coincides with that wave aberration coefficients differ from FOVs and perturbations. To keep optical performance, aberration field after compensation should remain unchanged. To realize it, NAT method (Eq. (5)) is derived. It can be seen that system recovery is only a special case of system compensation.

In the process of TM compensation, only linear term associated with aberration field decenter vector is considered. However, quadratic term associated with aberration field decenter vector also needs to be considered for the compensation of deformed PM, apart from linear term. After simulation, it is demonstrated that the aberration field induced from misaligned TM can be completely corrected by adjusting SM. But the aberration field induced from deformed PM can be partially corrected. It is concluded that PM can equip with the adjusting mechanism if necessary.

Optics EXPRESS

Compared the calculated correction values of SM based on NAT method with MFR method, it's found that the results are very close. It is proven that NAT method is reasonable. Apart from this comparison, NAT method is also compared with STM by Monte-Carlo simulations in the end. By comparison, it's found that NAT method here owns higher computation accuracy in larger perturbation ranges than STM. And NAT method is less sensitive to measurement errors. These are of great advantages than other methods.

Therefore, NAT method is applicable. The work in this paper facilitates the active optical compensation of the perturbed TMA telescopes, either on-axis or off-axis. It is meaningful for the development of active optics in astronomical telescopes.

## Funding

National Key Research and Development Program (2016YFF0103603).